Contribution from the Department of Chemistry,
University of Minnesota, Minneapolis, Minnesota 55455

Synthesis and Characterization of Cationic Gold-Rhodium Phosphite Cluster Complexes. X-ray Crystal and Molecular Structure of $\{Au_4Rh(H)_2[P(O\text{-}i\text{-}C_3H_7)_3]_2(PPh_3)_4\}PF_6$

Bruce D. Alexander, Ann M. Mueting, and Louis H. Pignolet*

Received August 8, 1989

The reactions of $Au(PPh_3)NO_3$ with $\{Rh(H)[P(OR)_3]_2\}_n$ (R = i-C_3H_7, n = 2; R = CH_3, n = 3) have been investigated. $\{Au_4Rh(H)_2[P(O\text{-}i\text{-}C_3H_7)_3]_2(PPh_3)_4\}PF_6$ (**1**) and $\{Au_5Rh(H)[P(OCH_3)_3]_2(PPh_3)_5\}PF_6$ (**2**) were synthesized by the reaction of $Au(PPh_3)NO_3$ and $\{Rh(H)[P(O\text{-}i\text{-}C_3H_7)_3]_2\}_2$ or $\{Rh(H)[P(OCH_3)_3]_2\}_3$, respectively, with THF as solvent. $\{Au_6Rh(H)[P(OCH_3)_3]_2(PPh_3)_6\}(PF_6)_2$ (**3**) was made by further reaction of $Au(PPh_3)NO_3$ and **2** with CH_2Cl_2 as solvent. Compound **1** was characterized by single-crystal X-ray diffraction in the solid state [**1**, $P\bar{1}$ (No. 2), a = 14.38 (1) Å, b = 14.50 (2) Å, c = 26.81 (2) Å, α = 101.98 (10)°, β = 89.03 (7)°, γ = 117.82 (10)°, T = -95 °C, Z = 2, R = 0.042 for 8,142 observations] and by ^{31}P and ^1H NMR spectroscopy in solution. The molecular structure of complex **1** consists of an approximately trigonal-bipyramidal (TBP) $RhAu_4$ core with a $Rh[P(O\text{-}i\text{-}C_3H_7)_3]_2$ unit occupying an equatorial position. The four $AuPPh_3$ units occupy the axial positions and the two remaining equatorial positions. The major deviation from ideal TBP geometry is reflected in the shorter Au-Rh distances (average 2.685 (1) Å) compared with the bonded Au-Au separations (average 2.904 (1) Å). The hydride ligands were not directly observed by X-ray diffraction in **1**; however, spectroscopic evidence, potential energy calculations, and the solid-state structural results (average distances: axial Au-Rh = 2.717 (1) Å; equatorial Au-Rh = 2.654 (1) Å) indicate the presence of one hydride bridging each of the longer Au-Rh bonds. Compounds **2** and **3** were characterized by IR and ^1H and ^{31}P NMR spectroscopies. Compounds **2** and **3** were each determined to possess one bridging hydride ligand.

Introduction

The synthesis and characterization of mixed-metal gold cluster compounds have incorporated the use of a wide variety of transition metals over the past few years.[1-30] Preparative methods have primarily involved reactions between anionic metal carbonyl clusters and $Au(PR_3)Cl$ or "$Au(PR_3)^+$" generated in situ and reactions between neutral metal carbonyl hydride clusters and $Au(PR_3)CH_3$, although several other synthetic routes have also been reported.[24,25] A variety of cationic transition-metal-gold cluster compounds have been prepared in our laboratory by reaction of $Au(PPh_3)NO_3$ with transition-metal phosphine complexes containing Ru, Os, Rh, Ir, Re, Pt, or Pd.[1,6-14] Many of these cluster compounds contain hydride ligands that bridge transition-metal-gold bonds. These compounds are important because of their intrinscially novel structures and properties, their potential use as bimetallic catalysts, and their potential to aid in understanding the role of gold in supported alloy catalysts.[31,32]

In this paper we report the synthesis, single-crystal X-ray analysis, and spectroscopic characterization of a new rhodium-gold compound, $\{Au_4Rh(H)_2[P(O\text{-}i\text{-}C_3H_7)_3]_2(PPh_3)_4\}PF_6$ (**1**), and the synthesis and spectroscopic characterization of $\{Au_5Rh(H)[P(OCH_3)_3]_2(PPh_3)_5\}PF_6$ (**2**), $\{Au_6Rh(H)[P(OCH_3)_3]_2(PPh_3)_6\}(PF_6)_2$ (**3**), and $\{Au_5Rh(H)_2[P(O\text{-}i\text{-}C_3H_7)_3(PPh_3)_5]^{2+}$ (**4**). The molecular structure of compound **1** is similar to that of the previously characterized iridium-gold complex, $[Au_4Ir(H)_2(PPh_3)_6]BF_4$ (**5**).[14]

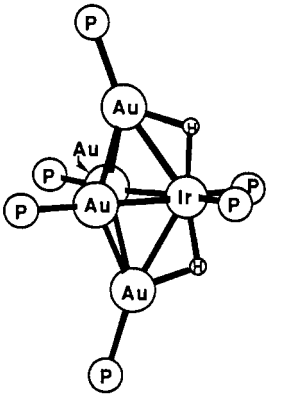

5

Both consist of an approximately trigonal-bipyramidal (TBP) core with one hydride bridging each of the axial M-Au bonds, as

(1) Mueting, A. M.; Bos, W.; Alexander, B. D.; Boyle, P. D.; Casalnuovo, J. A.; Balaban, S.; Ito, L. N.; Johnson, S. M.; Pignolet, L. H. Recent Advances in Di- and Polynuclear Chemistry. *New J. Chem.* **1988**, *12*, 505 and references cited therein.
(2) Jones, P. G. *Gold Bull.* **1986**, *19*, 46 and references cited therein.
(3) Braunstein, P.; Rosé, J. *Gold Bull.* **1985**, *18*, 17.
(4) Hall, K. P.; Mingos, D. M. P. *Prog. Inorg. Chem.* **1984**, *32*, 237 and references cited therein.
(5) Jones, P. G. *Gold Bull.* **1983**, *16*, 114 and references cited therein.
(6) Ito, L. N.; Sweet, J. D.; Mueting, A. M.; Pignolet, L. H.; Schoondergang, M. F. J.; Steggerda, J. J. *Inorg. Chem.* **1989**, *28*, 3696.
(7) Ito, L. N.; Johnson, B. J.; Mueting, A. M.; Pignolet, L. H. *Inorg. Chem.* **1989**, *28*, 2026.
(8) Boyle, P. D.; Boyd, D. C.; Mueting, A. M.; Pignolet, L. H. *Inorg. Chem.* **1988**, *27*, 4424.
(9) Alexander, B. D.; Gomez-Sal, M. P.; Gannon, P. R.; Blaine, C. A.; Boyle, P. D.; Mueting, A. M.; Pignolet, L. H. *Inorg. Chem.* **1988**, *27*, 3301.
(10) Boyle, P. D.; Johnson, B. J.; Alexander, B. D.; Casalnuovo, J. A.; Gannon, P. R.; Johnson, S. M.; Larka, E. A.; Mueting, A. M.; Pignolet, L. H. *Inorg. Chem.* **1987**, *26*, 1346.
(11) Alexander, B. D.; Boyle, P. D.; Johnson, B. J.; Johnson, S. M.; Casalnuovo, J. A.; Mueting, A. M.; Pignolet, L. H. *Inorg. Chem.* **1987**, *26*, 2547.
(12) Alexander, B. D.; Johnson, B. J.; Johnson, S. M.; Casalnuovo, A. L.; Pignolet, L. H. *J. Am. Chem. Soc.* **1986**, *108*, 4409.
(13) Boyle, P. D.; Johnson, B. J.; Buehler, A.; Pignolet, L. H. *Inorg. Chem.* **1986**, *25*, 5.
(14) Casalnuovo, A. L.; Casalnuovo, J. A.; Nilsson, P. V.; Pignolet, L. H. *Inorg. Chem.* **1985**, *24*, 2554.
(15) Kanters, R. P. F.; Schlebos, P. P. J.; Bour, J. J.; Bosman, W. P.; Behm, H. J.; Steggerda, J. J. *Inorg. Chem.* **1988**, *27*, 4034.
(16) Bour, J. J.; Kanters, R. P. F.; Schlebos, P. P. J.; Steggerda, J. J. *Recl. Trav. Chim. Pays-Bas* **1988**, *107*, 211.
(17) Manojlović-Muir, L.; Muir, K. W.; Treurnicht, I.; Puddephatt, R. J. *Inorg. Chem.* **1987**, *26*, 2418.
(18) Albinati, A.; Lehner, H.; Venanzi, L. M.; Wolfer, M. *Inorg. Chem.* **1987**, *26*, 3933.
(19) Murray, H. H.; Briggs, D. A.; Garzón, G.; Raptis, R. G.; Porter, L. C.; Fackler, J. P., Jr. *Organometallics* **1987**, *6*, 1992.
(20) Teo, B. K.; Hong, M.; Zhang, H.; Huang, D.; Shi, X. *J. Chem. Soc., Chem. Commun.* **1988**, 204.
(21) Low, A. A.; Lauher, J. W. *Inorg. Chem.* **1987**, *26*, 3863.
(22) Fumagalli, A.; Martinengo, S.; Albano, V. G.; Braga, D. *J. Chem. Soc., Dalton Trans.* **1988**, 1237.
(23) Albinati, A.; Janser, P.; Rhodes, L. F.; Venanzi, L. M. Personal communication.
(24) Bruce, M. I.; Nicholson, B. K. *J. Chem. Soc., Chem. Commun.* **1982**, 1141.
(25) van der Velden, J. W. A.; Bour, J. J.; Otterloo, B. F.; Bosman, J. H.; Noordik, J. H. *J. Chem. Soc., Chem. Comm.* **1981**, 583.
(26) Albinato, A.; Anklin, C.; Janser, P.; Lehner, H.; Matt, D.; Pregosin, P. S.; Venanzi, L. M. *Inorg. Chem.* **1989**, *28*, 1105.
(27) Albinato, A.; Demartin, F.; Janser, P.; Rhodes, L. F.; Venanzi, L. M. *J. Am. Chem. Soc.* **1989**, *111*, 2115.
(28) Douglas, G.; Jennings, M. C.; Manojlovic-Muir, L.; Puddephatt, J. *Inorg. Chem.* **1988**, *27*, 4516.
(29) Dearing, V.; Drake, S. R.; Johnson, B. F. G.; Lewis, J.; McPartlin, M.; Powell, H. R. *J. Chem. Soc., Chem. Commun.* **1988**, 1331.
(30) King, C.; Heinrich, D. D.; Garzon, G.; Wang, J.-C.; Fackler, J. P. *J. Am. Chem. Soc.* **1989**, *111*, 2300.
(31) Sinfelt, J. H. *Bimetallic Catalysts*; Wiley: New York, 1983; Chapters 1 and 2.
(32) Evans, J.; Jingxing, G. *J. Chem. Soc., Chem. Commun.* **1985**, 39.

0020-1669/90/1329-1313$02.50/0

evidenced by spectroscopic characterization and potential energy calculations. Compounds **1–4** represent the first rhodium–gold cluster complexes reported that contain phosphite ligands. They also demonstrate the effect of the phosphite steric requirement on the extent of cluster growth.

Experimental Section

Physical Measurements and Reagents. ^1H and ^{31}P NMR spectra were recorded at 300 and 121.5 MHz, respectively, with use of a Nicolet NT-300 spectrometer. ^{31}P NMR spectra were run with proton decoupling and are reported in parts per million (ppm) relative to the internal standard trimethyl phosphate (TMP), with positive shifts downfield. NMR simulations were carried out with the use of the Nicolet program NMCSIM.[33] Infrared spectra were recorded on a Perkin Elmer 1710 FT-IR spectrometer. Conductivity measurements were made with use of a Yellow Springs Model 31 conductivity bridge. Compound concentrations used in the conductivity experiments were 3×10^{-4} M in CH_3CN. FABMS experiments were carried out with use of a VG Analytical, Ltd., 7070E-HF high-resolution double-focusing mass spectrometer equipped with a VG 11/250 data system.[10] Microanalyses were carried out by Analytische Laboratorien, Fritz-Pregl-Strasse 24, D-5270 Gummersbach 1 Elbach, West Germany. Solvents were dried and distilled prior to use. $Au(PPh_3)NO_3$[34] was prepared as described in the literature. $\{Rh(H)[P(O\text{-}i\text{-}C_3H_7)_3]_2\}_2$,[35] and $\{Rh(H)[P(OCH_3)_3]_2\}_3$[35] were prepared as described in the literature, except (2-Me-allyl)Rh(COD)[36] was used instead of (allyl)Rh(COD). NH_4PF_6 was purchased from Aldrich Chemical Co. All manipulations were carried out under a purified N_2 atmosphere with use of standard Schlenk or dry box (Braun, Innovative Technologies) techniques unless otherwise noted.

Preparation of Compounds. $\{Au_4Rh(H)_2[P(O\text{-}i\text{-}C_3H_7)_3]_2(PPh_3)_4\}PF_6$ (1) was prepared by reaction of a THF solution of $\{Rh(H)[P(O\text{-}i\text{-}C_3H_7)_3]_2\}_2$ (10 mL, 433 mg, 0.416 mmol of dimer) with a THF solution of $Au(PPh_3)NO_3$ (5 mL, 457 mg, 0.876 mmol). An immediate reaction took place as indicated by a color change from green to brown and the precipitation of a brown product. After the mixture was stirred for 1 h, the THF was removed in vacuo, and the residue was redissolved in CH_2Cl_2. A MeOH solution containing 660 mg of NH_4PF_6 was added to this solution. A brownish orange product precipitated, which was collected and washed with Et_2O. The brownish orange product was redissolved in a minimal amount of CH_2Cl_2, and the solution was filtered and concentrated to ca. 4 mL. Upon the addition of ca. 2 mL of Et_2O, a green solid precipitated (identified to be $Au_9(PPh_3)_8^{3+}$ by ^{31}P NMR, δ 54.8), which was removed upon filtration. Further addition of Et_2O to this orange solution precipitated a bright orange solid, which was collected, washed with Et_2O, and dried under vacuum (237 mg, 46% yield based on Au). Recrystallization from a CH_2Cl_2/Et_2O solvent mixture at ambient temperature produced clear orange crystals suitable for X-ray diffraction. ^{31}P NMR (acetone-d_6, 25 °C): δ 196.9 (P_{Rh}, d of pentets, $J_{Rh\text{-}P_{Rh}}$ = 186.2 Hz and $J_{P_{Rh}\text{-}P_{Au}}$ = 58.2 Hz, intensity = 1), 40.6 (P_{Au}, t of d, $J_{P_{Au}\text{-}P_{Rh}}$ = 58.2 Hz and $J_{P_{Au}\text{-}Rh}$ = 12.4 Hz, intensity = 2). ^1H NMR in hydride region (CD_2Cl_2, 25 °C): δ −5.6 (pseudosextet, $J_{P_{Au}\text{-}H}$ = 17.7 Hz, $J_{P_{Rh}\text{-}H}$ = 0 Hz, and $J_{Rh\text{-}H}$ = 16.6 Hz, intensity = 2). Equivalent conductance (CH_3CN): 94.7 cm^2 mho mol^{-1}. FABMS (*m*-nitrobenzyl alcohol matrix): *m/z* 2355 ($(Au_4Rh(H)_2[P(O\text{-}i\text{-}C_3H_7)_3]_2(PPh_3)_4 = M)^+$), 2147 ($(M - P(O\text{-}i\text{-}C_3H_7)_3 - 2H)^+$). Anal. Calcd for $Au_4RhC_{90}H_{103}O_6P_7F_6$: C, 43.20; H, 4.15; P, 8.66. Found: C, 43.04; H, 4.01; P, 8.29.

$\{Au_5Rh(H)[P(OCH_3)_3]_2(PPh_3)_5\}PF_6$ (2) was prepared by reaction of a THF solution of $\{Rh(H)[P(OCH_3)_3]_2\}_3$ (10 mL, 380 mg, 0.360 mmol) with a THF solution of $Au(PPh_3)NO_3$ (5 mL, 566 mg, 1.085 mmol). After the mixture was stirred for 1.5 h, the color of the solution changed from brown to orange-brown. The THF was removed in vacuo, and the residue was dissolved in a minimal amount of CH_2Cl_2. A MeOH solution containing 700 mg of NH_4PF_6 was added to this CH_2Cl_2 solution. A bright orange product precipitated, which was collected, washed with cold MeOH followed by Et_2O, and dried under vacuum (436 mg, 75% yield based on Au). ^{31}P NMR (CD_2Cl_2, 25 °C): δ 211.6 (P_{Rh}, d of sextets, $J_{Rh\text{-}P_{Rh}}$ = 199.8 Hz and $J_{P_{Rh}\text{-}P_{Au}}$ = 60.5 Hz, intensity = 2), 38.4 (P_{Au}, t of d, $J_{P_{Au}\text{-}P_{Rh}}$ = 60.5 Hz and $J_{P_{Au}\text{-}Rh}$ = 11.9 H, intensity = 5). ^1H NMR in hydride region (CD_2Cl_2, 25 °C): δ −2.5 (multiplet, $J_{P_{Au}\text{-}H}$ = 17.5 Hz, $J_{P_{Rh}\text{-}H}$ = 0 Hz, and $J_{Rh\text{-}H}$ = 20.1 Hz, intensity = 1). Equivalent conductance (CH_3CN): 85.9 cm^2 mho mol^{-1} is indicative of a 1:1 electrolyte. FABMS (*m*-nitrobenzyl alcohol matrix): *m/z* 2648 ($(Au_5Rh(H)[P(OCH_3)_3]_2(PPh_3)_5 = M)^+$), 2385 ($(M - PPh_3)^+$), 2261 ($(M - PPh_3 - P(OCH_3)_3)^+$), 2123 ($(M - 2PPh_3)^+$).

$\{Au_6Rh(H)[P(OCH_3)_3]_2(PPh_3)_6\}(PF_6)_2$ (3) was prepared by reaction of $\{Au_5Rh(H)[P(OCH_3)_3]_2(PPh_3)_5\}PF_6$ (**2**) (193 mg, 0.0568 mmol) with $Au(PPh_3)NO_3$ (74 mg, 0.143 mmol) in 5 mL of CH_2Cl_2. There was an immediate color change from orange to orangish red. After the mixture was stirred for 1 h, the CH_2Cl_2 was removed in vacuo and the residue redissolved in a minimal amount of CH_2Cl_2. A MeOH solution containing 150 mg of NH_4PF_6 was added to this solution. An orangish red precipitate formed, which was collected, washed with toluene followed by Et_2O, and dried under vacuum (226 mg, 92% yield). ^{31}P NMR (acetone-d_6, 25 °C): δ 185.3 (P_{Rh}, d of septets, $J_{Rh\text{-}P_{Rh}}$ = 191.0 Hz and $J_{P_{Rh}\text{-}P_{Au}}$ = 48.3 Hz, intensity = 2), 40.9 (P_{Au}, t of d, $J_{P_{Au}\text{-}P_{Rh}}$ = 48.3 Hz and $J_{P_{Au}\text{-}Rh}$ = 12.0 Hz, intensity = 6). ^1H NMR in hydride region (acetone-d_6, 25 °C): δ −3.4 (mulitplet, $J_{P_{Au}\text{-}H}$ = 12.6 Hz, $J_{P_{Rh}\text{-}H}$ = 21.8 Hz, and $J_{Rh\text{-}H}$ = 20.1 Hz determined by selective ^{31}P decoupling, intensity = 1). Equivalent conductance (CH_3CN): 200.3 cm^2 mho mol^{-1} is indicative of a 1:2 electrolyte. FABMS (*m*-nitrobenzyl alcohol matrix): *m/z* 3252 ($(Au_6Rh(H)[P(OCH_3)_3]_2(PPh_3)_6PF_6 = M + PF_6)^+$) (M = cluster cation), 2991 ($(M - PPh_3 + PF_6)^+$), 2866 ($(M - PPh_3 - P(OCH_3)_3 + PF_6)^+$), 2720 ($(M - PPh_3 - P(OCH_3)_3)^+$), 2647 ($(M - Au - PPh_3 - H)^+$), 2385 ($(M - Au - 2PPh_3)^+$), 2261 ($(M - Au - 2PPh_3 - P(OCH_3)_3)^+$), 2123 ($(M - Au - 3PPh_3)^+$). Anal. Calcd for $Au_6RhC_{114}H_{109}O_6P_{10}F_{12}$: C, 40.30; H, 3.23; P, 9.12. Found: C, 40.33; H, 3.23; P, 9.13.

Reaction of $\{Au_4Rh(H)_2[P(O\text{-}i\text{-}C_3H_7)_3]_2(PPh_3)_4\}PF_6$ (1), $\{Au_5Rh(H)[P(OCH_3)_3]_2(PPh_3)_5\}PF_6$ (2), and $\{Au_6Rh(H)[P(OCH_3)_3]_2(PPh_3)_6\}(PF_6)_2$ (3) with CO. Samples of compounds **1–3** (ca. 30 mg) were each placed in an NMR tube, and CH_2Cl_2 (0.5 mL) was added. CO was bubbled through the solutions for 30 min, and then the samples were allowed to stand for 1 h. ^{31}P NMR spectra were recorded at 25 °C and all showed only signals corresponding to the respective starting cluster.

Reaction of $\{Au_4Rh(H)_2[P(O\text{-}i\text{-}C_3H_7)_3]_2(PPh_3)_4\}PF_6$ (1), $\{Au_5Rh(H)[P(OCH_3)_3]_2(PPh_3)_5\}PF_6$ (2), and $\{Au_6Rh(H)[P(OCH_3)_3]_2(PPh_3)_6\}(PF_6)_2$ (3) with PPh_3. In general, the reactants were mixed under N_2, and spectra were recorded after a reaction time of 1–2 h. Each sample of compound **1**, **2**, or **3** (ca. 30 mg) and 5 equiv of PPh_3 was placed in an NMR tube and CH_2Cl_2 (0.5 mL) was added. The samples were allowed to stand at ambient temperature for 1 h, and then the ^{31}P NMR spectra were recorded at 25 °C. Each reaction showed only resonances corresponding to the respective starting cluster along with free PPh_3 at ca. δ −6.0.

Reaction of $\{Au_4Rh(H)_2[P(O\text{-}i\text{-}C_3H_7)_3]_2(PPh_3)_4\}PF_6$ (1) with $Au(PPh_3)NO_3$. Preparation of $\{Au_5Rh(H)_2[P(O\text{-}i\text{-}C_3H_7)_3]_2(PPh_3)_5\}^{2+}$ (4). Compound **1** (36.9 mg, 0.0147 mmol) and $Au(PPh_3)NO_3$ (16.7 mg, 0.0320 mmol) were placed in a Schlenk tube and degassed. CD_2Cl_2 (0.5 mL) was added and the dark organge solution allowed to stir for 1 h. The solution was transferred to an NMR tube and a ^{31}P NMR spectrum

Table I. Crystallographic Data for $\{Au_4Rh(H)_2[P(O\text{-}i\text{-}C_3H_7)_3]_2(PPh_3)_4\}PF_6 \cdot 0.75CH_2Cl_2$ (**1**·0.75CH_2Cl_2)

Crystal Parameters and Measurement of Intensity Data	
space group	$P\bar{1}$ (No. 2)
cell params at *T*, °C	−95
a, Å	14.38 (1)
b, Å	14.50 (2)
c, Å	26.81 (2)
α, deg	101.98 (10)
β, deg	89.03 (7)
γ, deg	117.82 (10)
V, Å^3	4820 (20)
Z	2
calcd density, g cm^{-3}	1.78
abs coeff, cm^{-1}	64.0
max, min, av transm factors	1.00, 0.62, 0.82
formula	$C_{90.75}H_{105.5}Cl_2F_6O_6P_7Au_4Rh$
fw	2584.56
radiation	Mo Kα (λ = 0.71069 Å) graphite monochromatized

Refinement by Full-Matrix Least-Squares Techniques			
no. of params	558	R_w[a]	0.051
R[a]	0.042		

[a] The function minimized was $\sum w(|F_o| - |F_c|)^2$, where $w = 1/[\sigma(F_o)]^2$. The unweighted and weighted residuals are defined as $R = \sum(||F_o| - |F_c||)/\sum|F_o|$ and $R_w = [(\sum w(|F_o| - |F_c|)^2)/(\sum w|F_o|^2)]^{1/2}$. The error in an observation of unit weight (GOF) is $[\sum w(|F_o| - |F_c|)^2/(NO - NV)]^{1/2}$, where NO and NV are the number of observations and variables, respectively.

(33) NMCSIM is described in the Nicolet Magnetics Corp. 1280 program manual.
(34) Malatesta, J.; Naldini, L.; Simonetta, G.; Cariati, F. *Coord. Chem. Rev.* **1966**, *1*, 255.
(35) Sivak, A. J.; Muetterties, E. L. *J. Am. Chem. Soc.* **1979**, *101*, 4878.
(36) Fryzuk, M. D. *Inorg. Chem.* **1982**, *21*, 2134.

Table II. Positional Parameters and Their Estimated Standard Deviations for Core Atoms in $\{Au_4Rh(H)_2[P(O\text{-}i\text{-}C_3H_7)_3]_2(PPh_3)_4\}PF_6 \cdot 0.75CH_2Cl_2$ (**1**·0.75CH_2Cl_2)

atom	*x*	*y*	*z*	B,[a] Å^2
Au1	0.15551 (4)	−0.07865 (4)	0.27296 (2)	1.21 (1)
Au2	0.21986 (4)	−0.00783 (4)	0.17606 (2)	1.30 (1)
Au3	0.33231 (4)	0.05905 (4)	0.34550 (2)	1.20 (1)
Au4	0.31279 (4)	0.15213 (4)	0.26639 (2)	1.25 (1)
Rh	0.35032 (7)	−0.01400 (7)	0.24554 (4)	1.03 (2)
P1	−0.0201 (3)	−0.1664 (3)	0.2874 (1)	1.35 (8)
P2	0.1290 (3)	0.0002 (3)	0.1101 (1)	1.44 (8)
P3	0.3380 (3)	0.1145 (3)	0.4320 (1)	1.28 (8)
P4	0.3060 (3)	0.3101 (2)	0.2826 (1)	1.38 (8)
P5	0.3532 (3)	−0.1694 (3)	0.2445 (1)	1.46 (8)
P6	0.4957 (3)	0.0858 (3)	0.2076 (1)	1.44 (8)

[a] Atoms were refined anisotropically with the isotropic equivalent thermal parameters given.

recorded at 25 °C: δ 167.1 (P_{Rh}, d of sextets, $J_{P_{Rh}-P_{Au}}$ = 49.1 Hz, $J_{P_{Rh}-Rh}$ = 177.2 Hz, intensity = 2), 38.6 (P_{Au}, t of d, $J_{P_{Au}-P_{Rh}}$ = 49.1 Hz, $J_{P_{Au}-Rh}$ = 10.2 Hz, intensity = 5) and signals due to $\{Au_4Rh(H)_2[P(O\text{-}i\text{-}C_3H_7)_3]_2(PPh_3)_4\}^+$ (cation of **1**) (δ 196.9, 40.6), $[Au_9(PPh_3)_8]^{3+}$ (δ 54.8), $[Au(PPh_3)_2]^+$ (δ 42.6), and $Au(PPh_3)NO_3$ (δ 24.9). ^1H NMR recorded in the hydride region (25 °C, CD_2Cl_2): δ −3.1 (pseudoseptet, intensity = 2) and a signal due to $\{Au_4Rh(H)_2[P(O\text{-}i\text{-}C_3H_7)_3]_2(PPh_3)_4\}^+$ (cation of **1**) (δ −5.6). The yield based on the integration of the ^{31}P signals was ca. 90%.

X-ray Structure Determination. Collection and Reduction of X-ray Data. A summary of crystal data is presented in Table I. Crystals of $\{Au_4Rh(H)_2[P(O\text{-}i\text{-}C_3H_7)_3]_2(PPh_3)_4\}PF_6$ (**1**) were found to lose solvent upon removal from a CH_2Cl_2–Et_2O solution. This solvent loss was rapid and caused single crystals to fracture. Therefore, an orange rectangular crystal of $\{Au_4Rh(H)_2[P(O\text{-}i\text{-}C_3H_7)_3]_2(PPh_3)_4\}PF_6 \cdot 0.75CH_2Cl_2$ (**1**·0.75CH_2Cl_2) was stabilized by quickly coating it with a viscous high-molecular-weight hydrocarbon and was secured on a glass fiber by cooling to −95 °C. The crystal class and space group were unambiguously determined by the Enraf-Nonius CAD4-SDP-PLUS peak search, centering, and indexing programs[37] and by successful solution and refinement of the structure (vide infra). The intensities of three standard reflections were measured every 1.5 h of X-ray exposure time during data collection, and no decay was observed. The data were corrected for Lorentz, polarization, and background effects. Empirical absorption corrections were applied for compound **1** by use of ψ-scan data and the program EAC.[37]

Solution and Refinement of the Structure. The structure was solved by conventional heavy-atom techniques. The metal atoms were located by Patterson syntheses. Full-matrix least-squares refinement and difference Fourier calculations were used to locate all remaining non-hydrogen atoms. The atomic scattering factors were taken from the usual tabulation,[38] and the effects of anomalous dispersion were included in F_c by using Cromer and Ibers' values of $\Delta f'$ and $\Delta f''$.[39] Corrections for extinction were applied. The cluster core atoms, the P atoms of the PF_6^- counterions, and the Cl atoms of the CH_2Cl_2 solvent molecule in **1** were refined with anisotropic thermal parameters. Hydrogen atoms were not located in the final difference Fourier map, and therefore none were included. The crystal of compound **1** contained one CH_2Cl_2 solvate molecule per cation that converged to give an occupancy factor of 0.75 upon refinement. One well-behaved PF_6^- anion was located on a center of symmetry, yielding an occupancy factor of 0.5 per cation. Another PF_6^- anion was located very near a center of symmetry and was disordered such that it converged to an occupancy factor of 0.5. Therefore, the overall formulation of compound **1** contains one PF_6^- counterion. The largest peak in the final difference Fourier map of **1** was ca. 1.8 e Å^{-3} and was located near the disordered PF_6^- anion. The final positional and thermal parameters of the refined atoms within the coordination core are given in Table II. An ORTEP drawing of the cation including the labeling scheme and selected distances is shown in Figure 1. Complete listings of thermal parameters, positional parameters, distances, angles, least-squares planes, and structure factor amplitudes are included as supplementary material.[40]

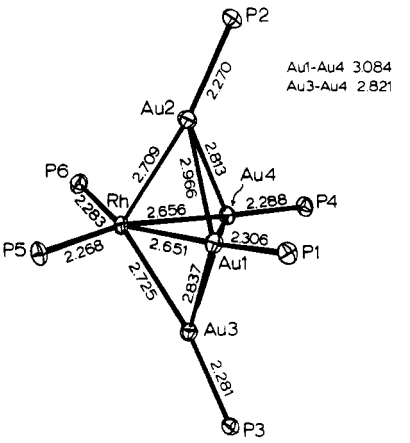

Figure 1. ORTEP drawing of the coordination core of **1** with selected bond distances (Å). Ellipsoids are drawn with 50% probability boundaries. Phenyl rings have been omitted for clarity. Esd's in the last significant figure for M–M and M–P distances are 1 and 3, respectively. Selected angles (deg), where the numbers refer to Au atoms are as follows: 1–Rh–2, 67.18 (3); 1–Rh–3, 63.68 (3); 1–Rh–4, 71.06 (3); 2–Rh–3, 115.60 (4); 2–Rh–4, 63.24 (3); 3–Rh–4, 63.24 (2); 1–Rh–P6, 155.2 (1); 4–Rh–P5, 164.61 (9); P5–Rh–P6, 106.2 (1); Rh–1–P1, 168.99 (9); Rh–1–4, 54.53 (2); 2–1–3, 104.79 (2); Rh–2–1, 55.48 (2); Rh–2–4, 57.45 (2); Rh–2–P2, 171.74 (9); Rh–3–1, 56.90 (2); Rh–3–4, 57.19 (2); Rh–3–P3, 170.99 (9); Rh–4–1, 54.40 (2); 2–4–3, 109.38 (2); Rh–4–P4, 171.57 (9).

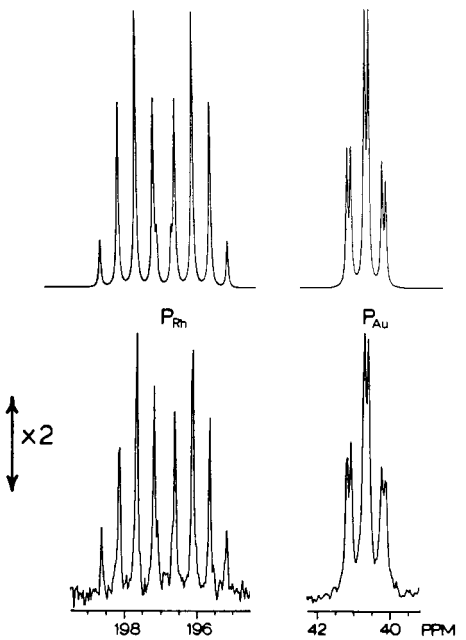

Figure 2. $^{31}P\{^1H\}$ NMR spectrum of $\{Au_4Rh(H)_2[P(O\text{-}i\text{-}C_3H_7)_3]_2(PPh_3)_4\}^+$ (cation of **1**), recorded at 25 °C with use of acetone-d_6 as the solvent (lower trace). Upper trace shows a ^{31}P NMR spectral simulation based on the coupling constants $J_{P_{Rh}-P_{Au}}$ = 58.2 Hz, $J_{P_{Rh}-Rh}$ = 186.2 Hz, and $J_{P_{Au}-Rh}$ = 12.4 Hz. The assignments of P_{Rh} and P_{Au} are discussed in the text.

Results

$\{Au_4Rh(H)_2[P(O\text{-}i\text{-}C_3H_7)_3]_2(PPh_3)_4\}PF_6$ (1). The addition of 2 equiv of $Au(PPh_3)NO_3$ to $\{Rh(H)[P(O\text{-}i\text{-}C_3H_7)_3]_2\}_2$ in a THF solution produced this cationic gold–rhodium compound as the nitrate salt. This product was then metathesized with NH_4PF_6 to give **1**. A single-crystal X-ray diffraction analysis of this compound was carried out in order to determine the nature of the gold–rhodium interactions and the overall structure of the complex. These questions could not be answered from the solution NMR

(37) All calculations were carried out on PDP 8A and 11/34 computers with use of the Enraf-Nonius CAD4-SDP programs. This crystallographic computing package is described by: Frenz, B. A. In *Computing in Crystallography*; Schenk, H., Olthoff-Hazekamp, R., van Koningsveld, H., Bassi, G. C., Eds.; Delft University Press: Delft, Holland, 1978; pp 64–71. *CAD 4 User's Manual*; Enraf-Nonius: Delft, Holland, 1978.

(38) Cromer, D. T.; Waber, J. T. In *International Tables for X-Ray Crystallography*; Kynoch: Birmingham, England, 1974; Vol. IV, Table 2.2.4.

(39) Cromer, D. T. In *International Tables for X-Ray Crystallography*; Kynoch: Birmingham, England, 1974; Vol. IV, Table 2.3.1.

(40) See paragraph at end of paper regarding supplementary material.

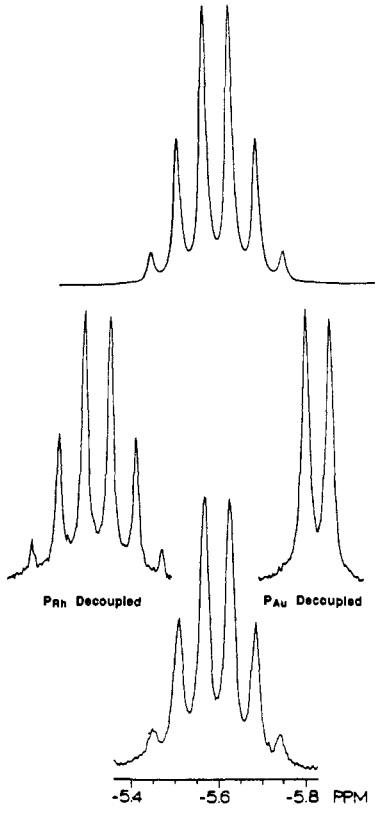

Figure 3. ^1H NMR spectrum of **1** in the hydride region recorded with use of CD_2Cl_2 as solvent at 25 °C shown with selective phosphorus decoupling. Upper trace is the ^1H NMR simulation based on the coupling constants $J_{P_{Au}-H}$ = 17.7 Hz, J_{Rh-H} = 16.6 Hz and $J_{P_{Rh}-H} \approx 0$ Hz.

and IR data alone (vide infra). The structure of the coordination core of the cation of **1** with selected distances and angles is shown in Figure 1. The ^{31}P NMR solution spectrum of **1** (25 °C, acetone-d_6) is in agreement with its solid-state structure. A trace of the spectrum is shown in Figure 2. Although the hydride ligands were not located in the X-ray structure of **1**, their presence was confirmed by the observation of a pseudosextet resonance at δ −5.6 in the room-temperature ^1H NMR spectrum recorded in the hydride region with CD_2Cl_2 as solvent (Figure 3). The formulation of **1** as a dihydride was based upon ^1H NMR integration data and the FABMS. The dihydride formulation is also consistent with the 1+ charge (one PF_6^- counterion per cluster) and the requirement that **1** is diamagnetic.

The positive ion FABMS analysis of **1** gave evidence for the presence of two hydride ligands. The major highest mass peak at m/z 2555 has an isotopic ion distribution pattern that closely matches that calculated for the parent cluster in $\{Au_4Rh(H)_2[P(O\text{-}i\text{-}C_3H_7)_3]_2(PPh_3)_4\}^+$.[10] Equivalent conductance measurements provided further support for the formulation of **1** as the 1:1 electrolyte $\{Au_4Rh(H)_2[P(O\text{-}i\text{-}C_3H_7)_3]_2(PPh_3)_4\}PF_6$.

$\{Au_5Rh(H)[P(OCH_3)_3]_2(PPh_3)_5\}PF_6$ (2). The addition of 3 equiv of $Au(PPh_3)NO_3$ to $\{Rh(H)[P(OCH_3)_3]_2\}_3$ in a THF solution produced this cationic gold–rhodium compound as the nitrate salt. This product was then metathesized with NH_4PF_6 to give **2**. This complex was characterized by solution ^{31}P and ^1H NMR spectroscopy (Experimental Section and vide infra) and by analysis of the positive ion FABMS. The positive ion FABMS analysis of **2** was important in the characterization of this compound and clearly showed the parent molecular ion ($M^+ = \{Au_5Rh(H)[P(OCH_3)_3]_2(PPh_3)_5\}^+$ and $(M - PPh_3)^+$ with the observed most abundant masses (m/z 2648.4 and 2385.3, respectively) within the experimental error of the calculated values (m/z 2648 and 2385, respectively) (see Experimental Section and Figure 4)). This result gives direct evidence for the presence of one hydride ligand.[10] Furthermore, no terminal hydride absorptions were observed in the IR spectrum of **2**. Equivalent conductance data provided further support for the formulation of **2** as the 1:1 electrolyte $\{Au_5Rh(H)[P(OCH_3)_3]_2(PPh_3)_5\}PF_6$.

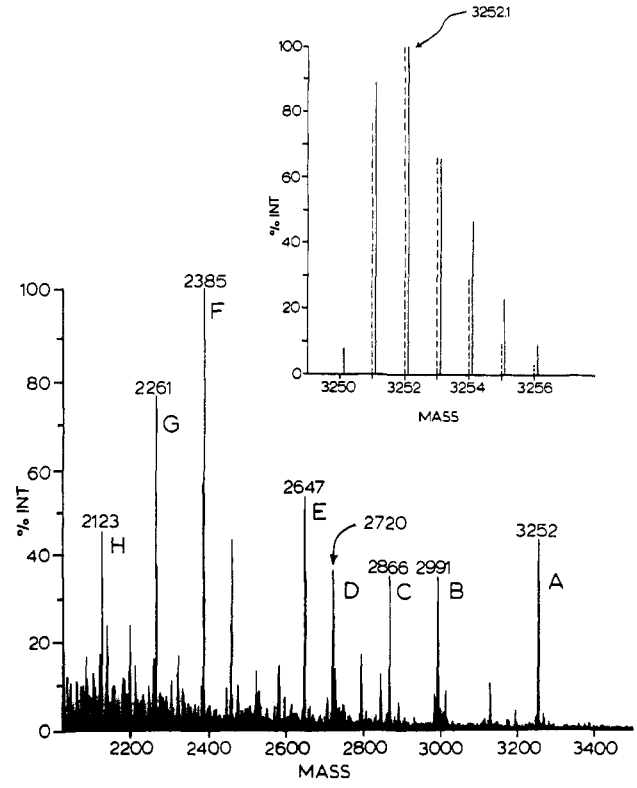

Figure 4. Positive ion FABMS (average 11 scans) of $\{Au_5Rh(H)[P(OCH_3)_3]_2(PPh_3)_5\}PF_6$ (**2**) in the m/z range 4000–2000, with a scan rate of 50 s/decade, 1:5000 resolution, and 3-kV accelerating voltage. The major peaks are assigned as follows, where M = $\{Au_5Rh(H)[P(OCH_3)_3]_2(PPh_3)_5\}$, and agree well with the calculated isotopic ion distribution patterns (see insert): A, M^+; B, $(M - PPh_3)^+$; C, $(M - PPh_3 - P(OCH_3)_3)^+$; D, $(M - 2PPh_3)^+$. Inset: observed (solid line) and simulated (dashed line) (VG ISO program) isotopic ion distributions for expanded peak A, $\{Au_5Rh(H)[P(OCH_3)_3]_2(PPh_3)_5\}^+$.

$\{Au_6Rh(H)[P(OCH_3)_3]_2(PPh_3)_6\}(PF_6)_2$ (3). The addition of an excess of $Au(PPh_3)NO_3$ to **2** in a CH_2Cl_2 solution produced this dicationic gold–rhodium compound as the nitrate salt. This product was then metathesized with NH_4PF_6 to give **3** and was characterized by solution ^{31}P and ^1H NMR spectroscopy (see Experimental Section and vide infra) and by analysis of the positive ion FABMS. The positive ion FABMS analysis of this compound gave a spectrum with well-resolved peaks, which is included as supplementary material.[40] An analysis of the isotopic ion distribution pattern for the highest mass peak gave a most abundant mass ion of 3252.1. A complete simulation of all isotopic combinations for the ion pair $\{Au_6Rh(H)[P(OCH_3)_3]_2(PPh_3)_6PF_6\}^+$ gave an isotopic ion distribution pattern that closely matched the observed pattern. An analysis of the fragmentation pattern (see supplementary material)[40] suggests that the neutral compound is $\{Au_6Rh(H)[P(OCH_3)_3]_2(PPh_3)_6\}(PF_6)_2$ (**3**). No terminal hydride absorptions were observed in the IR spectrum of **3**. Equivalent conductance and elemental analysis data provided further support for the formulation of **3** as the 1:2 electrolyte $\{Au_6Rh(H)[P(OCH_3)_3]_2(PPh_3)_6\}(PF_6)_2$.

Reactivity. $\{Au_4Rh(H)_2[P(O\text{-}i\text{-}C_3H_7)_3]_2(PPh_3)_4\}PF_6$ (**1**), $\{Au_5Rh(H)[P(OCH_3)_3]_2(PPh_3)_5\}PF_6$ (**2**), and $\{Au_6Rh(H)[P(OCH_3)_3]_2(PPh_3)_6\}(PF_6)_2$ (**3**) were found to be unreactive with CO in CH_2Cl_2. A CH_2Cl_2 solution of each cluster was saturated with CO and allowed to stand for 1 h. The ^{31}P NMR spectra of these reactions only had signals corresponding to the starting clusters. Compounds **1**–**3** were also found to be unreactive toward PPh_3. When 5 equiv of PPh_3 was added to CH_2Cl_2 solutions of **1**, **2**, or **3**, no reaction was observed as determined by observing the ^{31}P NMR. The only resonances seen were for the starting cluster and free PPh_3. There was no evidence for the extrusion of $AuPPh_3^+$ by the formation of $Au(PPh_3)_2^+$ as has been seen in many other MAu cluster complexes.[1,11] Furthermore, there was

no indication of rapid exchange of free PPh_3 with coordinated PPh_3 of the $AuPPh_3$ unit since the P_{Au}–P_{Rh} and P_{Au}–Rh coupling remained intact. PPh_3 also did not replace the phosphite ligands within several hours.

Since the reaction of an excess amount of $Au(PPh_3)NO_3$ with $\{Au_5Rh(H)[P(OCH_3)_3]_2(PPh_3)_5\}PF_6$ (**2**) in a CH_2Cl_2 solution produced $\{Au_6Rh(H)[P(OCH_3)_3]_2(PPh_3)_6\}(PF_6)_2$ (**3**) in good yield, a similar reaction was tried with **1**. When an excess (2.5 equiv) of $Au(PPh_3)NO_3$ was added to a CH_2Cl_2 solution of **1**, a darker orange solution was produced. Attempts to isolate this product as a solid, free of any unreacted **1**, were unsuccessful due to similar solubilities and properties of the two complexes. It was characterized in solution, however, by ^{31}P and ^1H NMR and by comparison of its NMR spectra to the NMR spectra of $\{Au_5Rh(H)[P(OCH_3)_3]_2(PPh_3)_5\}PF_6$ (**2**). The ^{31}P NMR spectrum for this product (25 °C, CD_2Cl_2) displayed a resonance at δ 167.1 assigned to the P_{Rh} atoms, which appeared as an overlapping doublet of sextets ($J_{P_{Rh}-P_{Au}}$ = 49.1 Hz and $J_{P_{Rh}-Rh}$ = 177.2 Hz), and a resonance at δ 38.6 assigned to the P_{Au} atoms, which appeared as a triplet of doublets ($J_{P_{Au}-Rh}$ = 10.2 Hz). The chemical shifts and coupling constants are shifted to lower values compared to those in **1**. This is consistent with an increase in coordination number at the rhodium center. The ^1H NMR (25 °C, CD_2Cl_2) recorded in the hydride region displayed a multplet resonance at δ −3.1, which appeared as a pseudoseptet due to coupling with five equivalent P_{Au} atoms and to the rhodium atom, similar to that of **2** (vide supra). These solution NMR results are consistent with the formulation of this compound as $\{Au_5Rh(H)_2[P(O\text{-}i\text{-}C_3H_7)_3]_2(PPh_3)_5\}^{2+}$ (**4**), which formed from the addition of $AuPPh_3^+$ to $\{Au_4Rh(H)_2[P(O\text{-}i\text{-}C_3H_7)_3]_2(PPh_3)_4\}^+$.

Discussion

X-ray Structural and Spectroscopic Analysis of $\{Au_4Rh(H)_2[P(O\text{-}i\text{-}C_3H_7)_3]_2(PPh_3)_4\}PF_6$ (1). The solid-state structure of **1** (Figure 1) consists of an approximately trigonal-bipyramidal (TBP) $RhAu_4$ core with Au2 and Au3 occupying the axial positions. This is analogous to the structure of $[Au_4Ir(H)_2(PPh_3)_6]BF_4$ (**5**).[14] As in **5**, the major deviation from ideal TBP geometry in **1** is reflected in the shorter Au–M distances (average 2.685 (1) Å in **1** and 2.693 (2) Å in **5**) compared with the bonded Au–Au separations (average 2.904 (1) Å in **1** and 2.917 (2) Å in **5**). In both **1** and **5** the equatorial Au–Au distance (labeled Au1–Au4 in **1**) is long (3.084 (1) Å in **1** and 3.142 (2) Å in **5**) and the Au–M–Au angle in the equatorial plane (71.06 (3)° in **1** and 72.33 (5)° in **5**) is larger than the equatorial M–Au–Au angles (54.53 (2) and 54.40 (2)° in 1 and 53.09 (4) and 54.58 (4)° in **5**).

The Au–PPh_3 vectors are approximately trans to the rhodiium atom (Rh–Au1–P1 168.99 (9)°, Rh–Au2–P2 171.74 (9)°, Rh–Au3–P3 170.99 (9)°, Rh–Au4–P4 171.57 (9)°), which is a general trend seen in most cluster complexes of this type.[1] The Au–Rh distances (average 2.685 (1) Å) are comparable to distances observed in other known rhodium–gold phosphine clusters (2.675 (3) Å in $[Au_3Rh(H)(CO)(PPh_3)_5]PF_6$[13] and 2.695 (2) Å in $[Au_3Rh(H)_2(triphos)(PPh_3)_3](CF_3SO_3)_2$[23]), but shorter than those in $[Rh_6C(CO)_{15}\{Au(PPh_3)\}_2]$ (average 2.824 (1) Å).[22] The Au–Au and Au–P distances (average 2.904 (1) and 2.286 (3) Å, respectively) are similar to those found in $[Au_3Rh(H)(CO)(PPh_3)_5]PF_6$ (average 2.872 (2) and 2.26 (1) Å)[13] and in $[Au_3Rh(H)_2(triphos)(PPh_3)_3](CF_3SO_3)_2$ (2.888 (1) and 2.260 (5) Å).[23] The Rh–P distances (average 2.276 (3) Å) are long compared to the distances found in $\{Rh(H)[P(O\text{-}i\text{-}C_3H_7)_3]_2\}_2$ (average 2.167 (4) Å),[41] which could be a result of the higher coordination number in **1**.

Although the cluster core in **1** is similar to that found in **5**, there is one notable difference. In **5**, the four phosphorus atoms that are bonded to the metals Rh, Au1, and Au4 in the equatorial plane lie approximately within this plane. The deviations are only +0.05 (1), +0.11 (1), −0.02 (1), and +0.10 (1) Å from the M_3 plane.[14] In **1**, the phosphorus atoms that are bonded to the metals in the equatorial plane are significantly displaced from this plane. This is most pronounced for the phosphite phosphorus atoms on the Rh. The deivations of P1, P4, P5, and P6 from this plane are +0.194 (4), −0.033 (4), −0.326 (4), and +0.552 (4) Å, respectively.

The ^{31}P NMR solution spectrum (Figure 2) consists of two resonances (δ 196.9 and 40.6) with an intensity ratio of 1:2, respectively. The resonance at δ 196.9 is a doublet of pentets and is assigned to the two equivalent rhodium phosphite phosphorus atoms, P_{Rh}. These phosphorus atoms couple to the rhodium atom (J = 186.2 Hz) to give the large doublet splitting and to the four equivalent gold phosphine phosphorus atoms, P_{Au} (J = 58.2 Hz), to give the pentet splitting. The resonance at δ 40.6 is assigned to the four gold phosphine phosphorus atoms, P_{Au}, which couple to the two equivalent P_{Rh} atoms to give a triplet and to the Rh atom (J = 12.4 Hz) to give the smaller doublet splitting. A selectively phosphorus-decoupled ^1H NMR experiment (vide infra and Figure 3) and a successful $^{31}P\{^1H\}$ NMR simulation confirmed this A_2X_4 assignment.

As for complex **5**, variable-temperature ^{31}P NMR experiments showed that **1** undergoes a rapid rearrangement in solution in which the axial and equatorial gold phosphine sites are interconverted. When a CH_2Cl_2–Freon-22 solution of **1** was cooled, both the P_{Rh} and P_{Au} resonances broadened. The slow-exchange limiting spectrum was reached at ca. −100 °C. This spectrum consisted of pseudotriplet centered at δ 198.8 due to the P_{Rh} atoms P5 and P6 ($J_{P_{Rh}-P_{Au}}$ = 197.5 Hz, $J_{P_{Rh}-Rh}$ = 186.2 Hz, intensity = 2), a broad singlet due to the P_{Au} atoms P2 and P3 (δ 42.2, intensity = 2), and an apparent broad doublet due to the P_{Au} atoms P1 and P4 (δ 37.3, $J_{P_{Au}-P_{Rh}}$ = 197.5 Hz, intensity = 2). ^{31}P NMR simulation studies showed this pattern to be consistent with an AA′BB′C_2 spin system in which $J_{A'-B}$ and $J_{A-B'}$ are equal to 197.5 Hz and are much greater in magnitude than the remaining spin–spin coupling constants, which are not resolved. The C atoms are the axial P2 and P3 atoms, and the A and B atoms are the equatorial P1, P4, P5, and P6 atoms. The solution variable-temperature NMR behavior of **1** is very similar to that found for **5**.[14]

The ^1H NMR spectrum of **1** is shown with selective phosphorus decoupling in Figure 3. These decoupling results support the above assignments of P_{Rh} and P_{Au} and yield all of the P_{Au}–H and Rh–H coupling constants. The multiplet was successfully simulated and is also shown in Figure 3.

Decoupling of the P_{Rh} atoms caused the hydride resonance to collapse to a somewhat sharper pseudosextet. This six-line pattern is due to similar coupling constants of the hydrides to the four equivalent P_{Au} atoms (17.7 Hz) and to the Rh center (16.6 Hz) and also indicates that $J_{P_{Rh}-H}$ is less than ca. 1 Hz. Decoupling of the P_{Au} atoms resulted in the collapse of the signal to a doublet due to coupling to the rhodium center. The very small $J_{P_{Rh}-H}$ value indicates a cisoid geometry between the phosphorus atoms on Rh and the hydride ligands.[12,18]

Typically, we find that the bridging $M(\mu\text{-}H)AuPPh_3$ coupling constants are greater than 20 Hz and terminal $HM\text{–}AuPPh_3$ coupling constants are less than 15 Hz.[1,12,14] The value of 17.7 Hz, however, is an average of all four P_{Au}–H coupling constants due to the rapid rearrangement of **1** in solution. Therefore, it is likely that the two hydrides occupy bridiging positions and that $J_{P_{Au}-H}$ for the bridging interaction is larger than 17.7 Hz. This phenomenon is also observed in the isostructural iridium–gold complex **5** ($J_{P_{Au}-H}$ = 13.5 Hz).[14] Additional support for this dihydride-bridged formulation can be inferred from a combination of solid-state structural data, potential energy calculations, and infrared spectroscopy. The axial Au–Rh distances (average 2.717 (1) Å) are significantly longer than the equitorial Au–Rh distances (average 2.654 (1) Å). This suggests that the hydrides are bridging the axial Au–Rh bonds since monohydrogen-bridged M–μ-H–M bonds are generally longer than nonbridged M–M bonds in these type of compounds.[12,42,43] Calculation of the optimum hydride

(41) Brown, R. K.; Williams, J. M.; Fredrich, M. F.; Day, V. W.; Sivak, A. J.; Muetterties, E. L. *Proc. Natl. Acad. Sci. U.S.A.* **1979**, *76*, 2099.

(42) Teller, R. G.; Bau, R. *Struct. Bonding (Berlin)* **1981**, *44*, 1.

positions in **1** with use of Orpen's potential energy minimization computer program[1,44] provided further verification that the two hydrides bridge the longer axial Au–Rh bonds in the solid state. Also, no terminal hydride absorptions were observed in the IR spectrum of **1**. On the basis of a similar analysis, complex **5** has been determined to possess a dihydride-bridged formulation with the hydrides bridging the longer axial Au–Ir bonds.[1,14]

NMR Spectroscopic Analysis of $\{Au_5Rh(H)[P(OCH_3)_3]_2(PPh_3)_5\}PF_6$ (2). The ^{31}P NMR solution spectrum of **2** (25 °C, CD_2Cl_2) consisted of two peaks (δ 211.6 and 38.4) with an intensity ratio of 2:5. The resonance at δ 211.6 appeared as a doublet of sextets and is assigned to the two equivalent rhodium phosphite phosphorus atoms, P_{Rh}. The P_{Rh} atoms couple to the Rh atom (J = 199.8 Hz) to give the large doublet splitting and to the five equivalent gold phosphine phosphorus atoms, P_{Au} (J = 60.5 Hz) to give the sextet splitting. The P_{Au} atoms (δ 38.4, triplet of doublets) couple to the two equivalent P_{Rh} atoms to give a triplet and to the Rh atom (J = 11.9 Hz) to give the smaller doublet splitting. A selectively phosphorus-decoupled ^1H NMR experiment (vide infra) confirmed this A_2X_5 assignment. Variable-temperature ^{31}P NMR experiments with CH_2Cl_2–Freon 22 as solvent showed that **2** undergoes a rapid rearrangement in solution in which all the five gold phosphine sites are interconverted. As the tempeature was lowered, both resonances began to broaden, and at −110 °C the P_{Rh} resonance had collapsed into a broad featureless peak, while the P_{Au} resonance had split into four broad singlets with relative intensity ratios of 1:1:2:1.

The ^1H NMR spectrum of **2** (25 °C, CD_2Cl_2) showed a multiplet centered at δ −2.5, which was consistent with an overlapping doublet of sextets, with J = 20.1 and 17.5 Hz for the doublet and sextet splittings, respectively. The integration of this signal relative to the phenyl hydrogens and the methyl hydrogens indicated the presence of only one hydride ligand. This was further supported by the FABMS analysis (vide supra). Selective phosphorus decoupling of **2** confirmed that the P_{Rh}–H coupling constant is ca. 0 Hz, and that the 20.1 Hz coupling is due to the hydride coupling to the Rh atom and the 17.5 Hz coupling is due to the hydride coupling to the five equivalent P_{Au} atoms. The P_{Au}–H coupling constant is an average of all five P_{Au}–H coupling constants due to the rapid rearrangement of **2** in solution. This causes the observed $J_{P_{Au}-H}$ to be smaller than what would normally be seen for a bridging $Ru(\mu\text{-}H)AuPPh_3$ coupling constant. Therefore, the value is consistent with a bridging hydride formulation. As in **1**, the very small $J_{P_{Rh}-H}$ indicates a cisoid geometry between the Rh phosphorus atoms and the hydride.

X-ray quality crystals could not be obtained for this compound so the structure of the Au_5Rh core is unknown. The low-temperature ^{31}P NMR spectrum (vide supra) shows that the compound has low or no symmetry. The only other well-characterized Au_5M cluster of this type is $[Au_5Re(H)_4(PPh_3)_7](PF_6)_2$.[1,13] This compound has an edge-shared bitetrahedral core geometry with approximate σ symmetry and shows three P_{Au} lines in the ^{31}P NMR spectrum with 1:2:2 relative intensities at low temperature.[13] Compound **2** must therefore have a lower symmetry not inconsistent with a ($RhAu_2$) face-capped adduct of **1**. Such a geometry would have five nonequivalent triphenylphosphine groups.

NMR Spectroscopic Analysis of $\{Au_6Rh(H)[P(OCH_3)_3]_2(PPh_3)_6\}(PF_6)_2$ (3). The ^{31}P NMR solution spectrum of **3** (25 °C, acetone-d_6) consisted of two resonances (δ 185.3 and 40.9) with an intensity ratio of 2:6. The resonance at δ 185.3, assigned as the two equivalent P_{Rh} atoms, appeared as a doublet of overlapping septets due to coupling of the rhodium atom (J = 191.0 Hz) and the six equivalent P_{Au} atoms (J = 48.3 Hz). The resonance at δ 40.9 was a triplet of doublets and is assigned to the six P_{Au} atoms. The P_{Au} atoms couple to the two equivalent P_{Rh} atoms to give a triplet and to the Rh atom (J = 12.0 Hz) to give the smaller doublet splitting. A selectively phosphorus-decoupled ^1H NMR experiment (vide infra) confirmed this A_2X_6 assignment. Variable-temperature ^{31}P NMR experiments with CH_2Cl_2–Freon 22 as solvent showed that **3** undergoes a rapid rearrangement in solution in which all the six gold phosphine sites are interconverted. As the temperature was lowered, both resonances began to broaden, and at −110 °C, the P_{Rh} resonance had collapsed into a broad featureless peak, while the P_{Au} resonance had split into four broad singlets with an intensity ratio of 1:3:1:1.

The ^1H NMR spectrum of **3** (25 °C, acetone-d_6) was recorded in the hydride region and displayed a multiplet resonance centered at δ −3.4. Unlike **1** and **2**, which had very similar ^1H NMR coupling constants, **3** possesses much different values. This difference is manifested by the fact that in **3** there is a significant coupling between the two equivalent P_{Rh} atoms and the bridging hydride ligand (J = 21.8 Hz). This coupling constant in **1** and **2** was too small to be observed. This value of 21.8 Hz for the H–Rh–$P(O\text{-}i\text{-}C_3H_7)_3$ coupling indicates that in **3** the $P(O\text{-}i\text{-}C_3H_7)_3$ groups are somewhat transoid to the bridging hydride. The $J_{P_{Rh}-H}$ value, however, is still smaller than what would be expected for a totally trans stereochemistry.[12,18] The P_{Au}–H and Rh–H coupling constants in **3** (12.6 and 20.1 Hz, respectively), however, are similar to the values seen in **1** and **2**. Compound **3** is stereochemically nonrigid at 25 °C, and therefore, the P_{Au}–H coupling constant is an average of all six P_{Au}–H couplings (vide supra) and is consistent with a $(\mu\text{-}H)AuPPh_3$ formulation.

The above data do not permit a determination of the geometry of the Au_6Rh core of **3**. Other Au_6M clusters of this type include $[Au_6Pt(CC\text{-}t\text{-}Bu)(PPh_3)_7]^+$ and $[Au_6Pt(CO)(PPh_3)_7]^{2+}$.[1,6,45] The former has a geometry that consists of a central platinum atom at the apex of two face-shared Au_4Pt square-based pyramids[45] while the latter has a structure in which the Pt atom and four Au atoms form a trigonal bipyramid sharing an edge with a tetrahedron formed by the Pt and three Au atoms.[6] Drawings of these structures are shown in Chart I with the *tert*-butyl group of the acetylide ligand and the phenyl groups omitted for clarity. Although these clusters both have 90 valence electrons, they have very different geometries. Compound **3** is isoelectronic with these clusters and therefore could have a structure similar to either one. Unfortunately, we do not have a clear understanding of the factors that influence geometry so a prediction is not possible. On the basis of the low-temperature P_{Au} ^{31}P NMR spectrum of **3** (vide supra), however, the lower symmetry structure of $[Au_6Pt(CO)(PPh_3)_7]^{2+}$ is the one preferred. In this compound the six P_{Au} atoms are nonequivalent while the acetylide derivative has approximate σ symmetry and should show three P_{Au} signals with intensities 2:2:1:1 in the low-temperature limit. The 1:3:1:1 four-line pattern of **3** is more consistent with the lower symmetry compound with some accidental overlapping signals. We are continuing our efforts to isolate a single crystal of **3** but thus far have been unsuccessful.

Chart I

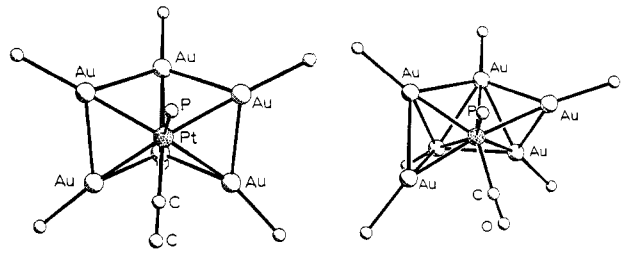

$[Au_6Pt(CC\text{-}t\text{-}Bu)(PPh_3)_7]^+$ $[Au_6Pt(CO)(PPh_3)_7]^{2+}$

Summary

Four new hydridorhodium–gold cluster compounds of the general type $[Rh(\mu\text{-}H)_x(phosphite)_2(AuPPh_3)_y]^{n+}$ have been

(43) Bau, R.; Teller, R. G.; Kirtley, S. W.; Koetzle, T. F. *Acc. Chem. Res.* **1979**, *12*, 176.

(44) Orpen, A. G. *J. Chem. Soc., Dalton Trans.* **1980**, 2509. The potential energy minimization calculations indicated that the hydrides occupied two bridging sites with potential energy values of 0.29 and −0.24. There were also sites capping the Au_2Rh faces; however, these were of higher potential energies.

(45) Smith, D. E.; Welch, A. J.; Treurnicht, I.; Puddephatt, R. J. *Inorg. Chem.* **1986**, *25*, 4617.

synthesized and characterized. These are the first examples that contain phosphite ligands. The larger triisopropyl phosphite ligand gave clusters with $y = 4$ and 5 while, with the smaller trimethyl phosphite ligand, clusters with $y = 5$ and 6 were formed. This is an expected trend based on steric crowding around the rhodium atom. The hydride ligands in these clusters are thought to be bridging the Ru–Au bonds. Although these compounds are unreactive toward small molecules such as CO, PPh_3, and H_2 and have not shown catalytic reactivity, they do serve to broaden the range of metal–gold cluster compounds. Work is continuing on these and related clusters in an effort to understand the factors that determine their novel structures.

Acknowledgment. This work was supported by the National Science Foundation (Grant NSF CHE-8818187) and the donors of the Petroleum Research Fund, administered by the American Chemical Society.

Supplementary Material Available: Figure S1, displaying the ORTEP drawing of **1**, Figure S2, showing the positive ion FABMS of **3**, Table S1, listing the complete crystal data and data collection parameters, and Tables S2–S6, listing general temperature factor expressions, final positional and thermal parameters for all atoms including solvate molecules, distances and angles, and least-squares planes (15 pages); Table S7, listing observed and calculated structure factor amplitudes (33 pages). Ordering information is given on any current masthead page.

Contribution from the Corporate Research Science Laboratories, Exxon Research and Engineering Company, Annandale, New Jersey 08801, and Department of Chemistry, University of California at Berkeley, and Materials and Chemical Sciences Division, Lawrence Berkeley Laboratory, Berkeley, California 94720

Models for Organometallic Polymers. Zigzag Chains of $Mo_2(O_2CCH_3)_4$ Units Linked by DMPE and TMED Ligands

Michael C. Kerby,*,† Bryan W. Eichhorn,*,‡ J. Alan Creighton,§ and K. Peter C. Vollhardt∥

Received April 28, 1989

Infinite zigzag chains of $Mo_2(O_2CCH_3)_4$ units linked by the bidentate ligands 1,2-bis(dimethylphosphino)ethane (dmpe) and tetramethylethylenediamine (tmed) crystallize from solutions of $Mo_2(O_2CCH_3)_4$ (**1**) dissolved in the respective *neat* ligand. Single-crystal X-ray structures of the light yellow polymers $^1_\infty[Mo_2(O_2CCH_3)_4(dmpe)]$ (**2**) and $^1_\infty[Mo_2(O_2CCH_3)_4(tmed)]$ (**3**) showed that the compounds were isostructural. Compound **2** crystallizes in space group $P\bar{1}$ (−135 °C) with $a = 8.473$ (2) Å, $b = 9.562$ (3) Å, $c = 7.654$ (3) Å, $\alpha = 110.59$ (2)°, $\beta = 100.06$ (2)°, $\gamma = 69.26$ (2)°, $Z = 1$, $V = 541.9$ (3) Å^3, $R = 0.058$, and $R_w = 0.058$. Compound **3** crystallizes in space group $P\bar{1}$ (20 °C) with $a = 8.388$ (1) Å, $b = 8.445$ (2) Å, $c = 8.840$ (2) Å, $\alpha = 105.95$ (2)°, $\beta = 115.62$ (1)°, $\gamma = 91.63$ (2)°, $Z = 1$, $V = 535.1$ (2) Å^3, $R = 0.025$, and $R_w = 0.033$. The ligands dmpe and tmed are coordinated axially through weak Mo–L bonds to relatively unperturbed $Mo_2(O_2CCH_3)_4$ centers. The solid-state Raman spectrum of **3** reveals a small decrease in the Mo–Mo stretching frequency ($\nu_{Mo-Mo} = 391$ cm^{-1}) relative to **1** ($\nu_{Mo-Mo} = 405$ cm^{-1}). TGA and powder X-ray diffraction studies involving **3** showed that solid-state thermolysis results in the expulsion of tmed at 92 °C and the formation of crystalline **1**.

Introduction

Interest in low-dimensional metal-containing polymers has been stimulated because of their potential to have the electrical and optical properties found in metals.[1] A severe impediment to the formation of oligomers from dinuclear metal complexes is the propensity of the latter to condense into metal clusters.[2] However, several bimetallic carboxylates, $M_2(O_2CR)_4$,[3] produce such polymers when treated with coordinating bidentate bases. For example, the addition of pyrazine (pyz) to aqueous solutions of dicopper(II) tetraacetate furnishes linear arrays of $Cu_2(O_2CCH_3)_4(pyz)$ units.[4] Similarly, an isomorphous pyrazine adduct of dichromium(II) tetraacetate was structurally characterized, revealing one-dimensional chains comprising $Cr_2(O_2CCH_3)_4(pyz)$ fragments.[5] Linear and zigzag chains of dirhodium(II) tetracarboxylates are produced with the bidentate ligands phenazine and durenediamine, respectively.[6] Recently, the structure of $Cu_2L_2(O_2CCH_3)_2 \cdot Cu_2(O_2CCH_3)_4 \cdot 2EtOH$ [where LH = *N*-methyl-*N'*-(4,6-dimethoxysalicylidene)-1,3-propanediamine] was reported in which alternating dicopper(II) subunits are linked through hydrogen bonds to form a one-dimensional array.[7] We were interested in assessing the effects of hydrogen bonding and ligand polarity in the synthesis of related one-dimensional compounds containing $Mo_2(O_2CCH_3)_4$ subunits.

Tertiary phosphines react with $M_2(O_2CCF_3)_4$ (M = Mo, W) to produce two classes of Lewis base adducts shown by I and II.[8-13]

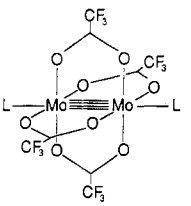

I

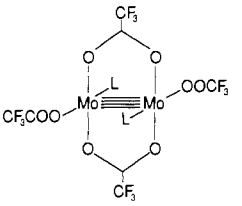

II

The preference for a particular structure type can be predicted rather well by analysis of phosphine cone angle and basicity values of the phosphine ligands. Spectroscopic studies have shown that the addition of bulky tertiary phosphines [i.e. $PMePh_2$, PPh_3,

† Exxon Research and Engineering Co. Present address: Exxon Research and Development Laboratories, P.O. Box 2226, Baton Rouge, LA 70821.
‡ Exxon Research and Engineering Co. Present address: Department of Chemistry and Biochemistry, University of Maryland, College Park, MD 20742.
§ Exxon Research and Engineering Co. Present address: Chemical Laboratories, University of Kent, Canterbury CT2 7NH, U.K.
∥ UC Berkeley.

(1) Miller, J. S. *Extended Linear Chain Compounds*; Plenum Press: New York, 1981–83; Vols. 1–3.
(2) Gates, B. C., Guczi, L., Knozinger, H., Eds. *Metal Clusters in Catalysis*; Elsevier: Amsterdam, 1986.
(3) Cotton, F. A.; Walton, R. A. *Multiple Bonds Between Metal Atoms*; John Wiley & Sons: New York, 1982.
(4) (a) Valentine, J. S.; Silverstein, A. J.; Soos, Z. G. *J. Am. Chem. Soc.* **1974**, *96*, 97. (b) Morosin, B.; Hughes, R. C.; Soos, Z. G. *Acta Crystallogr., Sect. B: Struct. Crystallogr. Cryst. Chem.* **1975**, *B31*, 762.
(5) Cotton, F. A.; Felthouse, T. R. *Inorg. Chem.* **1980**, *19*, 328.
(6) Cotton, F. A.; Felthouse, T. R. *Inorg. Chem.* **1981**, *20*, 600.
(7) Chiari, B.; Piovesana, O.; Tarantelli, T.; Zanazzi, P. F. *Inorg. Chem.* **1988**, *27*, 3246.
(8) Girolami, G. S.; Mainz, V. V.; Andersen, R. A. *Inorg. Chem.* **1980**, *19*, 805.
(9) Santure, D. J.; McLaughlin, K. W.; Huffman, J. C.; Sattelberger, A. P. *Inorg. Chem.* **1983**, *22*, 1877.
(10) Girolami, G. S.; Andersen, R. A. *Inorg. Chem.* **1982**, *21*, 1318.
(11) Cotton, F. A.; Lay, D. G. *Inorg. Chem.* **1981**, *20*, 935. With the ligand PPh_2Me, both class I and class II complexes are isolated; see this reference and ref 10.
(12) Hursthouse, M. B.; Malik, K. M. *Acta Crystallogr., Sect. B* **1979**, *B35*, 2709.
(13) Santure, D. J.; Sattelberger, A. P. *Inorg. Chem.* **1985**, *24*, 3477.

0020-1669/90/1329-1319$02.50/0